Draft version November 30, 2018
Typeset using LaTeX default style in AASTeX62

Discovery of three new transiting hot-Jupiters: WASP-161 b, WASP-163 b and WASP-170 b

K. Barkaoui,[1,2] A. Burdanov,[1] C. Hellier,[3] M. Gillon,[1] B. Smalley,[3] P. F. L. Maxted,[3] M. Lendl,[4,5] A. H. M. J. Triaud,[6] D. R. Anderson,[3] J. McCormac,[7] E. Jehin,[1] Y. Almleaky,[8,9] D. J. Armstrong,[7] Z. Benkhaldoun,[2] F. Bouchy,[5] D. J. A. Brown,[7] A. C. Cameron,[10] A. Daassou,[2] L. Delrez,[11,1] E. Ducrot,[1] E. Foxell,[7] C. Murray,[11] L. D. Nielsen,[5] F. Pepe,[5] D. Pollacco,[7] F. J. Pozuelos,[1] D. Queloz,[11,5] D. Segransan,[5] S. Udry,[5] S. Thompson,[11] and R. G. West[7]

[1] *Space sciences, Technologies and Astrophysics Research (STAR) Institute, Université de Liège, Belgium*
[2] *Oukaimeden Observatory, High Energy Physics and Astrophysics Laboratory, Cadi Ayyad University, Marrakech, Morocco*
[3] *Astrophysics Group, Keele University, Staffordshire, ST5 5BG, UK*
[4] *Space Research Institute, Austrian Academy of Sciences, Schmiedlstr. 6, 8042 Graz, Austria*
[5] *Observatoire astronomique de l'Université de Geneve, 51 ch. des Maillettes, 1290 Sauverny, Switzerland*
[6] *School of Physics & Astronomy, University of Birmingham, Edgbaston, Birmingham B15 2TT, United Kingdom*
[7] *Department of Physics, University of Warwick, Gibbet Hill Road, Coventry, CV4 7AL, UK*
[8] *Space and Astronomy Department, Faculty of Science, King Abdulaziz University, 21589 Jeddah, Saudi Arabia*
[9] *King Abdullah Centre for Crescent Observations and Astronomy, Makkah Clock, Mecca 24231, Saudi Arabia*
[10] *School of Physics and Astronomy, University of St Andrews, North Haugh, St Andrews, Fife KY16 9SS*
[11] *Cavendish Laboratory, J J Thomson Avenue, Cambridge, CB3 0HE, UK*

ABSTRACT

We present the new discovery of three new transiting hot-Jupiters by the WASP-South project, WASP-161 b, WASP-163 b and WASP-170 b. Follow-up radial velocities obtained with the Euler/CORALIE spectrograph and transit light-curves obtained with the TRAPPIST-North, TRAPPIST-South, SPECULOOS-South, NITES, and Euler telescopes have enabled us to determine the masses and radii for these transiting exoplanets. WASP-161 b completes an orbit around its $V = 11.1$ F6V-type host star in 5.406 days, and has a mass $M_p = 2.5 \pm 0.2 M_{Jup}$ and radius $R_p = 1.14 \pm 0.06\ R_{Jup}$. WASP-163 b orbiting around its host star (spectral type G8V and the magnitude $V = 12.5$) each 1.609 days, and has a mass $M_P = 1.9 \pm 0.2\ M_{Jup}$ and a radius $R_p = 1.2 \pm 0.1\ R_{Jup}$. WASP-170 b has a mass of $1.7 \pm 0.2\ M_{Jup}$ and a radius of $1.14 \pm 0.09\ R_{Jup}$, is on a 2.344 days orbit around a G1V-type star of magnitude $V = 12.8$. Given their irradiations ($\sim 10^9$ erg.s^{-1}.cm^{-2}) and masses, the three new planets' sizes are in the good agreement with classical models of irradiated giant planets.

Keywords: planetary systems- stars: WASP-161, WASP-163 and WASP-170- techniques: photometric, radial velocities and spectroscopic

1. INTRODUCTION

Inaugurated by the seminal discovery of 51 Peg b in 1995 (Mayor and Queloz 1995), the study of exoplanets has dramatically developed to become one of the most important fields of modern astronomy. Since 1995, the number of exoplanets detected, most of them by the transit technique (Charbonneau et al. 2000; Henry et al. 2000).

Among this large harvest, highly irradiated giant planets (aka hot Jupiters) transiting bright nearby stars have a particular scientific interest. These rare objects - $< 1\%$ of solar-type stars (Winn and Fabrycky 2015) - undergo irradiation orders of magnitude larger than any solar system planets (Fortney et al. 2007), and are also subject to intense gravitational and magnetic fields (Correia and Laskar 2010; Chang et al. 2010). Studying in detail their physical and chemical response to such extreme conditions provides a unique opportunity to improve our knowledge on planetary structure, composition and physics. The brightness of their host star combined to their eclipsing configuration makes

Corresponding author: K. Barkaoui
khalid.barkaoui@doct.uliege.be

possible such detailed characterization, notably to measure precisely their size, mass, and orbital parameters (Winn 2010; Deming and Seager 2009), but also to probe their atmospheric properties, for example the $P-T$ profiles, chemical composition and albedos (Seager and Deming 2010; Sing et al. 2016; Crossfield 2015).

The WASP (Wide Angle Search for Planets) project (described in Pollacco et al. (2006); Collier Cameron et al. (2007))uses two robotic installations, one at La Palma (Spain) and one at Sutherland (South Africa), to scout the sky for gas giants transiting the solar type stars. With more than 100 hot Jupiters discovered so far in front of bright nearby stars, WASP is a key contributor to the study of highly irradiated giant planets. In this paper, we report the discovery of three new gas giants, WASP-161 b, WASP-163 b and WASP-170 b, transiting bright ($V=$ 11.1, 12.5 & 12.8) solar-type (F6-, G8- and G1-type) dwarf stars.

In Section 2, we present the observations used to discover WASP-161 b, WASP-163 b and WASP-170 b, and to confirm their planetary natures and measure their parameters. In Section 2.2.1, we describe notably TRAPPIST-North, a 60cm robotic telescope installed recently by the University of Liège at Oukaimeden observatory (Morocco), that played a significant role in the confirmation and characterization of the planets. Section 3.1 presents the determination of the atmospheric parameters of the host stars. In Section 3.2, we describe our global analysis of the dataset for the three planetary systems that enabled us to determine their main physical and orbital parameters. We discuss briefly our results in Section 6.

2. OBSERVATIONS AND DATA REDUCTION

2.1. *WASP photometry*

WASP-161 and WASP-170 (see Table 1 for coordinates and magnitudes) were observed with the WASP-South (Hellier et al. 2011, 2012) in 2011 and 2012, while WASP-163 was observed in 2010 and 2012. The WASP-South data reduction methods described by Collier Cameron et al. (2006), and selected (Collier Cameron et al. 2007) as valuable candidates showing possible transits of short-period ($\sim$ 5.4, 1.6, and 2.3 days) planetary sizes bodies (Fig. 1).

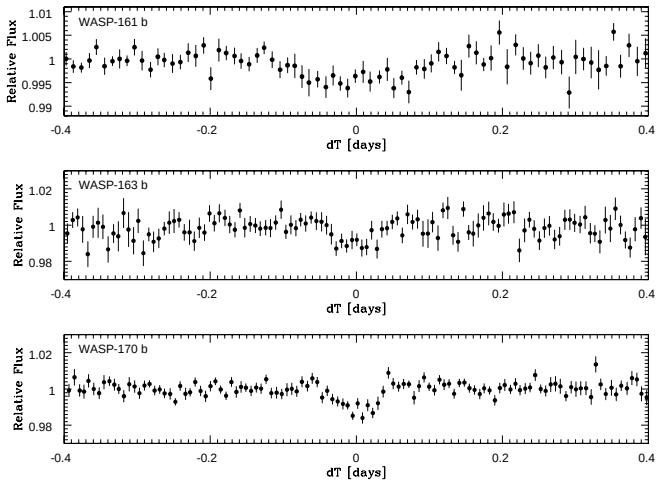

Figure 1. The light curve of WASP-161 (*top*), WASP-163 (*middle*) and WASP-170 (*bottom*) (binned = 10 min) folded on the transit ephemeris from the transit search algorithm described in Collier Cameron et al. (2006).

2.2. *Follow-up Photometry*

2.2.1. *TRAPPIST-North*

TRAPPIST-North is a new robotic telescope of 60-cm diameter installed in June 2016 at Oukaimeden Observatory (Morocco). It is installed by the University of Liège (Belgium) and in collaboration with the Cadi Ayyad University of Marrakech (Morocco). TRAPPIST-North extends the TRAPPIST project to the Northern hemisphere, and, as its Southern twin TRAPPIST-South, aims to the detection and characterization of transiting exoplanets, and the study of comets and other small bodies (e.g. asteroids) in the Solar System. The exoplanet program of TRAPPIST (75%

	Star general informations		
	WASP-161	WASP-163	WASP-170
	2MASS08252108-1130035	2MASS17060901-1024467	2MASS09013992-2043133
	GaiaId 5751177091580191360	GaiaId 4334991786994866304	GaiaId 5656184406542140032
RA (J200)	$08^h25^m21.09^s$	$17^h06^m08.98^s$	$09^h01^m39.93^s$
Dec (J200)	$-11°30'03.6''$	$-10°24'47.0''$	$-20°43'13.6''$
Vmag [UCAC4]	10.98	12.54	12.65
Jmag [2MASS]	10.09	10.67	11.13
Gmag [Gaia-DR1]	10.84	12.13	12.36
Parallax [mas] [*Gaia*-DR2]	2.8864 ± 0.0345	3.7981 ± 0.0525	3.2439 ± 0.0390
	Stellar parameters from spectroscopic analysis		
T_{eff} (K)	6400 ± 100	5500 ± 200	5600 ± 150
$\log g_\star$ [cgs]	4.5 ± 0.15	4.0 ± 0.3	4.0 ± 0.2
$[Fe/H]$	$+0.16 \pm 0.09$	-0.34 ± 0.21	$+0.22 \pm 0.09$
Spectral type	F6	G8	G1
$V \sin i$ [Km/s]	18 ± 0.8	< 5	5.6 ± 1
$\log A(Li)$	No Lithium seen	< 1.6	1.52 ± 0.09
	Parameters from MCMC analysis		
MCMC Jump parameters			
$(R_p/R_\star)^2$ [%]	0.45092 ± 0.00023	1.417 ± 0.067	1.382 ± 0.001
Impact parameter b [$R_\star$]	$0.14^{+0.15}_{-0.10}$	$0.45^{+0.09}_{-0.06}$	0.689 ± 0.021
Transit duration W [d]	0.2137 ± 0.0022	0.093 ± 0.001	0.085 ± 0.001
Mid-transit T_0 [HJD]	7416.5289 ± 0.0011	7918.4620 ± 0.0004	7802.3915 ± 0.0002
Orbital period P [d]	5.4060425 ± 0.0000048	1.6096884 ± 0.0000015	2.34478022 ± 0.0000036
RV K_2 [m.s^{-1}d$^{1/3}$]	405 ± 20	386.69 ± 16	340 ± 20
Effective temperature T_{eff} [K]	6406 ± 100	5499 ± 200	5593 ± 150
Metallicity $[Fe/H]$	0.16 ± 0.09	-0.34 ± 0.21	0.21 ± 0.19
Deduced stellar parameters from MCMC			
Mean density $\rho_\star$ [$\rho_\odot$]	$0.282^{+0.013}_{-0.027}$	$0.92^{+0.13}_{-0.10}$	$1.121^{+0.093}_{-0.076}$
Stellar surface gravity $\log g_\star$ [cgs]	$4.111^{+0.023}_{-0.033}$	$4.411^{+0.042}_{-0.040}$	4.466 ± 0.031
Stellar mass $M_\star$ [$M_\odot$]	1.39 ± 0.14	0.97 ± 0.15	0.93 ± 0.15
Stellar radius $R_\star$ [$R_\odot$]	$1.712^{+0.083}_{-0.072}$	$1.015^{+0.071}_{-0.074}$	$0.938^{+0.056}_{-0.061}$
Luminosity $L_\star$ [$L_\odot$]	$4.44^{+0.56}_{-0.48}$	$0.84^{+0.20}_{-0.17}$	0.77 ± 0.14
Deduced planet parameters from MCMC	WASP-161 b	WASP-163 b	WASP-170 b
RV K [ms^{-1}]	230 ± 12	329 ± 14	255 ± 15
Planet/star radius ratio $R_p/R_\star$	0.0671 ± 0.0017	0.119 ± 0.003	0.1175 ± 0.0041
Impact parameter b [$R_\star$]	$0.14^{+0.15}_{-0.10}$	$0.448^{+0.063}_{-0.094}$	0.689 ± 0.021
Semi-major axis $a/R_\star$	$8.49^{+0.13}_{-0.28}$	$5.62^{+0.26}_{-0.21}$	$7.71^{+0.21}_{-0.18}$
Orbital semi-major axis a [AU]	0.0673 ± 0.0023	0.0266 ± 0.0014	0.0337 ± 0.0018
Inclination i_p [deg]	$89.01^{+0.69}_{-1.0}$	$85.42^{+1.10}_{-0.85}$	84.87 ± 0.28
Density ρ_p [ρ_{Jup}]	1.66 ± 0.22	$1.07^{+0.23}_{-0.17}$	$1.21^{+0.24}_{-0.19}$
Surface gravity $\log g_p$ [cgs]	$3.69^{+0.37}_{-0.42}$	3.52 ± 0.05	3.54 ± 0.05
Mass M_p [M_{Jup}]	2.49 ± 0.21	1.87 ± 0.21	1.6 ± 0.2
Radius R_p [R_{Jup}]	$1.143^{+0.065}_{-0.058}$	1.202 ± 0.097	1.096 ± 0.085
Roche limit a_R [AU]	$0.01101^{+0.00075}_{-0.00068}$	0.011 ± 0.001	0.011 ± 0.001
a/a_R	$6.12^{+0.25}_{-0.28}$	$2.35^{+0.16}_{-0.13}$	3.15 ± 0.19
Equilibrium temperature T_{eq} [K]	1557^{34}_{-29}	1638 ± 68	1422 ± 42
Irradiation [erg.s^{-1}.cm^{-2}]	$1.35^{+0.34}_{-0.26} \times 10^9$	$1.63 \pm 0.45 \times 10^9$	$9.3^{+2.3}_{-2.5} \times 10^8$

Table 1. The parameters of the WASP-161, WASP-163, and WASP-170 planetary systems (values + 1σ error bars), as deduced from our data analysis presented in Section 3

of its observational time) is dedicated to several programs: participating to the SPECULOOS project that aims to explore the nearest ultracool dwarf stars for transiting terrestrial planets (Gillon et al. 2017; Gillon 2018; Burdanov et al. 2017; Delrez et al. 2018); the search for the transit of planets previously detected by radial velocity (Bonfils et al. 2011); the follow-up of transiting planets of high interest (e.g. Gillon et al. 2012); and the follow-up of transiting planet candidates identified by wide-field transit surveys like WASP (e.g. Delrez et al. 2014). TRAPPIST-North has a F/8 Ritchey-Chretien optical design and protected by a 4.2 meters diameter dome equipped with a weather station and independent rain and light sensors. The telescope is equipped with a thermoelectrically-cooled 2048×2048 deep-depletion Andor IKONL BEX2 DD CCD camera that has a pixel scale of 0.60" that translates into a FOV of 19.8' × 19.8'. It is coupled to a direct-drive mount of German equatorial design. For more technical details and performances of the TRAPPIST telescopes described in Jehin et al. (2011).

TRAPPIST-North observed two partial transits of WASP-161 b in the Sloan-z' filter (20 Dec 2017 and 12 Feb 2018), two partial transits and one full transit of WASP-163 b in the $I + z$ filter (24 Apr, 02 May, and 13 Jun 2017), and three partial transits of WASP-170 b in the $I + z$ (19 Apr 2017 and 11 Jan 2018) and V (17 Feb 2017) filters. The reduction and photometric analysis of the data were performed as described in Gillon et al. (2013). The resulting light curves are shown in figures 2, 3, and 4.

2.2.2. *TRAPPIST-South*

We used the 60cm robotic telescope TRAPPIST-South (TRansiting Planets and PlanetesImals Small Telescope; Gillon et al. 2011; Jehin et al. 2011) at La Silla (Chile) to observe a partial transit of WASP-161 b in the Sloan-z' filter on 28 Jan 2016, two partial transits of WASP-163 b in a broad $I + z$ filter on 6 Sep 2014 and 5 July 2016, and two transits (one full + one partial) of WASP-170 b in $I + z$ on 25 Dec 2015 and 26 Feb 2017. TRAPPIST-South is equipped with a thermoelectrically-cooled 2K × 2K CCD with the pixel scale of 0.65" that translates into a 22' × 22' of FOV. Standard calibration of the images, fluxes extraction and differential photometry were then performed as described in Gillon et al. (2013). The resulting light curves are shown in figures 2, 3, and 4.

2.2.3. *EulerCam*

We used the EulerCam camera (Lendl et al. 2012) on the 1.2-m Euler-Swiss telescope at La Silla Observatory in Chile to observe a transit of WASP-163 b on 27 July 2016 in the RG filter, and also a transit of WASP-170 b on 20 Dec 2016 in the broad NGTS filter ($\lambda_{NGTS} = [500 - 900nm]$, Wheatley et al. 2017). The calibration and photometric reduction (aperture + differential photometry) of the images were performed as described by Lendl et al. (2012). The resulting light curves are shown in figures 3 and 4.

2.2.4. *NITES*

We use 0.4-m NITES (Near-Infrared Transiting ExoplanetS Telescope, McCormac et al. 2014) robotic telescope at La Palma (Canary Islands) to observe two transits of WASP-163 b. The first transit was full and observed in R-band on 27 June 2016, while the second was only partial and observed in I-band on 10 July 2016. NITES is equipped with a 1024×1024 CCD camera that has a pixel scale of 0.66″ that translates into a FOV of 11.3' × 11.3'. The standard calibration of the science images, fluxes extraction and differential photometry were then performed as described in Craig et al. (2015); Barbary (2016); Bertin and Arnouts (1996); McCormac et al. (2013). The resulting light curves are shown in figure 3.

2.2.5. *SPECULOOS-South*

We use 1-m robotic SSO-Europa telescope, one of the four telescopes of the SPECULOOS-South facility, (more details found in Delrez et al. (2018); Gillon (2018); Burdanov et al. (2017)) to observe one full-transit of WASP-161 b on 5 Jan 2018 in the Sloan-z' filter. Each 1-m robotic telescope equipped with 2K×2K CCD camera, with good sensitivities in the very-near-infrared up to 1 μm. The calibration and photometric reduction of the data were performed as described in Gillon et al. (2013). The resulting light curve is shown in figure 2.

2.3. *Follow-up spectroscopy*

We gathered series of spectra of the three stars with the CORALIE spectrograph (Queloz et al. 2000) mounted on the 1.2-meter Euler-Swiss telescope at ESO La Silla Observatory in Chile. An exposure time of 30 min was used for each of these spectroscopic observations. We measured 24 spectra of WASP-161 between December 2014 and January

2017; 25 spectra of WASP-163 between June 2015 and May 2017; and 20 spectra of WASP-170 between February 2015 and May 2017. We applied the cross correlation technique described in Baranne et al. (1996) on the spectra of each star to measure the radial velocities (RVs) presented in Table 6. The resulting RV time-series show clear sinusoidal signals with periods and phases in good agreement with those deduced from the WASP transit detections (Fig. 2, 3, and 4).

For each star, the bisector spans (BS, Queloz et al. 2001) of the cross correlation functions (CCF) have standard deviations close to their average errors (122 *vs* 80 ms^{-1}, 116 *vs* 125 ms^{-1} and 87 *vs* 97 ms^{-1} for WASP-161, WASP-163 and for WASP-170 respectively). Furthermore, a linear regression analysis do not show any significant correlation with between these BS and the corresponding RVs, the computed slopes being -0.02 ± 0.16, 0.07 ± 0.09, and 0.01 ± 0.11 for, respectively, WASP-161, WASP-163 and WASP-170 (Fig. 2, 3, and 4). This absence of correlation enables us to discard the scenario of a blended eclipsing binary (BEB). Indeed, if the orbital signal of a BEB was causing a clear periodic wobble of the sum of its CCF(s) and the one of the target, then it should also create a significant periodic distortion of its shape, resulting in variations of the BS in phase with those of the RV, and with the same order of magnitude Torres et al. (2004).

3. DATA ANALYSIS

3.1. *Spectroscopic analysis*

For each host star, we co-added the CORALIE spectra to produce a combined spectrum with an average S/N per pixel between 50 and 100. We analyzed each combined spectrum with the technique described by Doyle et al. (2013) to determine the following stellar atmospheric parameters: the effective temperature T_{eff}, the surface gravity $\log g$, the lithium abundance $\log A(\mathrm{Li})$, the metallicity $[Fe/H]$, and the projected rotational velocity $v \sin i$. $v \sin i$ was constrained using the calibration of Doyle et al. (2014), assuming macroturbulence values of 5.31 $\mathrm{km.s}^{-1}$, 3.59 $\mathrm{km.s}^{-1}$ and 3.74 $\mathrm{km.s}^{-1}$ for WASP-161, WASP-163 and WASP-170 respectively. The results of this spectral analysis are shown in Table 1.

3.2. *RVs + light curves analysis*

We performed a global analysis of the RVs (Table 6) and transit light curves (Table 3) with the MCMC (Markov-Chain Monte Carlo) algorithm described by Gillon et al. (2012) to determinate the parameters of each planetary system. While the CORALIE RVs were modeled with a classical Keplerian model (e.g. Murray and Correia 2010), the transit light curves were represented by the transit model of Mandel and Agol (2002), assuming a quadratic limb-darkening law, multiplied by a baseline model consisting of a polynomial function of one or several external parameters (time, background, airmass, etc., see Table 3). The selection of the model used for each time-series was based on the minimization of the Bayesian Information Criterium (BIC, Schwarz 1978).

TRAPPIST-North and TRAPPIST-South telescopes are equipped with German equatorial mounts that have to rotate of 180° at meridian, resulting in different positions of the stars' images on the detector after the flip, translating into an offset of the fluxes in the light curves. For the corresponding light curves, a normalization offset at the time of the flip was thus added to the assumed model (Table 3).

For each system, the "jump" parameters of the Markov Chains, i.e. the parameters perturbed at each step of the chains, were the transit duration, depth, and impact parameter (W, dF and b, respectively), the orbital period P, the mid-transit time T_0, the parameters $\sqrt{e}\cos\omega$ and $\sqrt{e}\sin\omega$ (with ω the argument of periastron and e the orbital eccentricity), the parameter $K2 = K\sqrt{1-e^2}P^{1/3}$ (with K is the RV semi-amplitude), and the stellar metallicity $[Fe/H]$ and effective temperature T_{eff}. In addition, for each filter, the combinations, $c_1 = 2\times u_1 + u_2$ and $c_2 = u_1 - 2\times u_2$ were also jump parameters, u_1 and u_2 being the linear and quadratic limb-darkening coefficients. Normal prior probability distribution functions (PDFs) based on the theoretical tables of Claret (2000) were assumed for u_1 and u_2 (Table 5). For T_{eff} and $[Fe/H]$, gaussian PDFs based on the values + errors derived from our spectral analysis (Table 1) were used. For the other jump parameters, uniform prior PDFs were assumed (e.g. $e \geq 0$, $b \geq 0$).

Each global analysis was composed of three Markov Chains of 10^5 steps whose convergence was checked using the statistical test presented by Gelman and Rubin (1992). The correlation of the noise present in the light curves was taken into account by rescaling the errors as described by Gillon et al. (2012). For the RVs, the quadratic difference between the mean error of the measurements and the standard deviation of the best-fit residuals were computed as 32.6 $\mathrm{m.s}^{-1}$, 54.1 $\mathrm{m.s}^{-1}$, and 42.8 $\mathrm{m.s}^{-1}$ for WASP-161, WASP-163 and WASP-170, respectively. These 'jitter' noises were added quadratically to the errors.

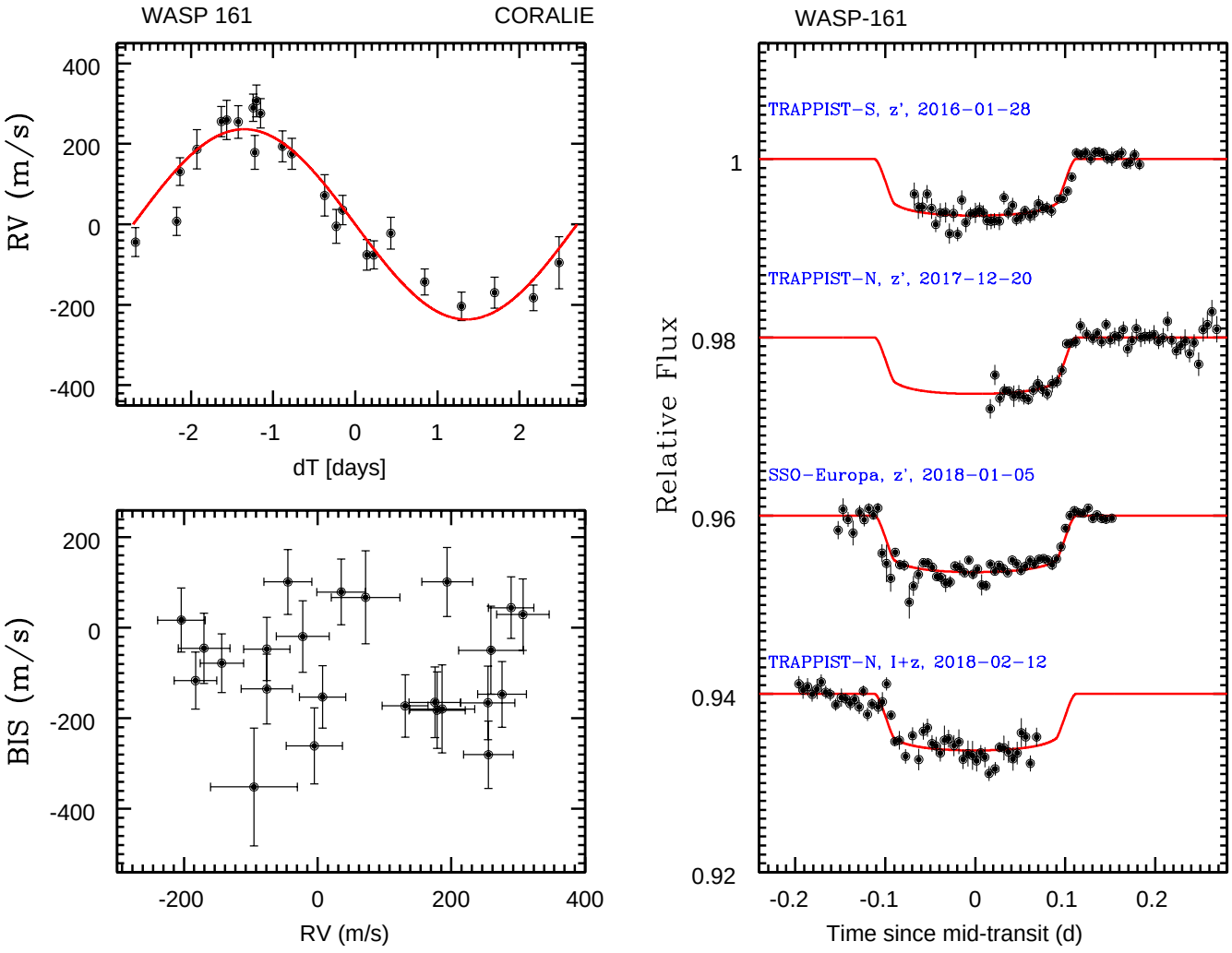

Figure 2. *Right-hand panel*: Individual follow-up transit light curves for WASP-161 binned per 0.005d (7.2min). The solid red lines are the best-fit transit models. We shifted the light curves along the y axis for clarity. *Left-hand panel, top*: CORALIE RVs for WASP-161 with the best-fit Keplerian model in red. *Left-hand panel, bottom*: bisector spans (BIS) *vs* RVs diagram.

At each step of the Markov chains, a value for the stellar density ρ_* was computed from dF, b, W, P, $\sqrt{e}\cos\omega$, and $\sqrt{e}\sin\omega$ (see, e.g., Winn 2010). This value of ρ_* was then used in combination with the values for T_{eff} and $[Fe/H]$ to compute a value for the stellar mass M_* from the empirical calibration of (Enoch et al. 2010). Two MCMC analyses were performed for each system, one assuming an eccentric orbit and one assuming a circular one. The Bayes factors, computed as $\exp(-\Delta BIC/2)$, were largely (> 1000) in favor of a circular model for the three systems, and we thus adopted the circular solution for all of them. These solutions are presented in Table 1. The non-circular solutions enable us to estimate the 3σ upper limits on the orbital eccentricity as 0.43, 0.13 and 0.23 for respectively, WASP-161 b, WASP-163 b and WASP-170 b.

As a sanity check of our results, we also estimated the stellar radius $R_\star$ from the star's parallax determined by Gaia (Gaia Collaboration et al. 2018), its effective temperature T_{eff}, and its bolometric magnitude M_{bol}, using the equations:

$$M_v = V_{mag} - 5\log_{10}(d/10), \quad (1)$$

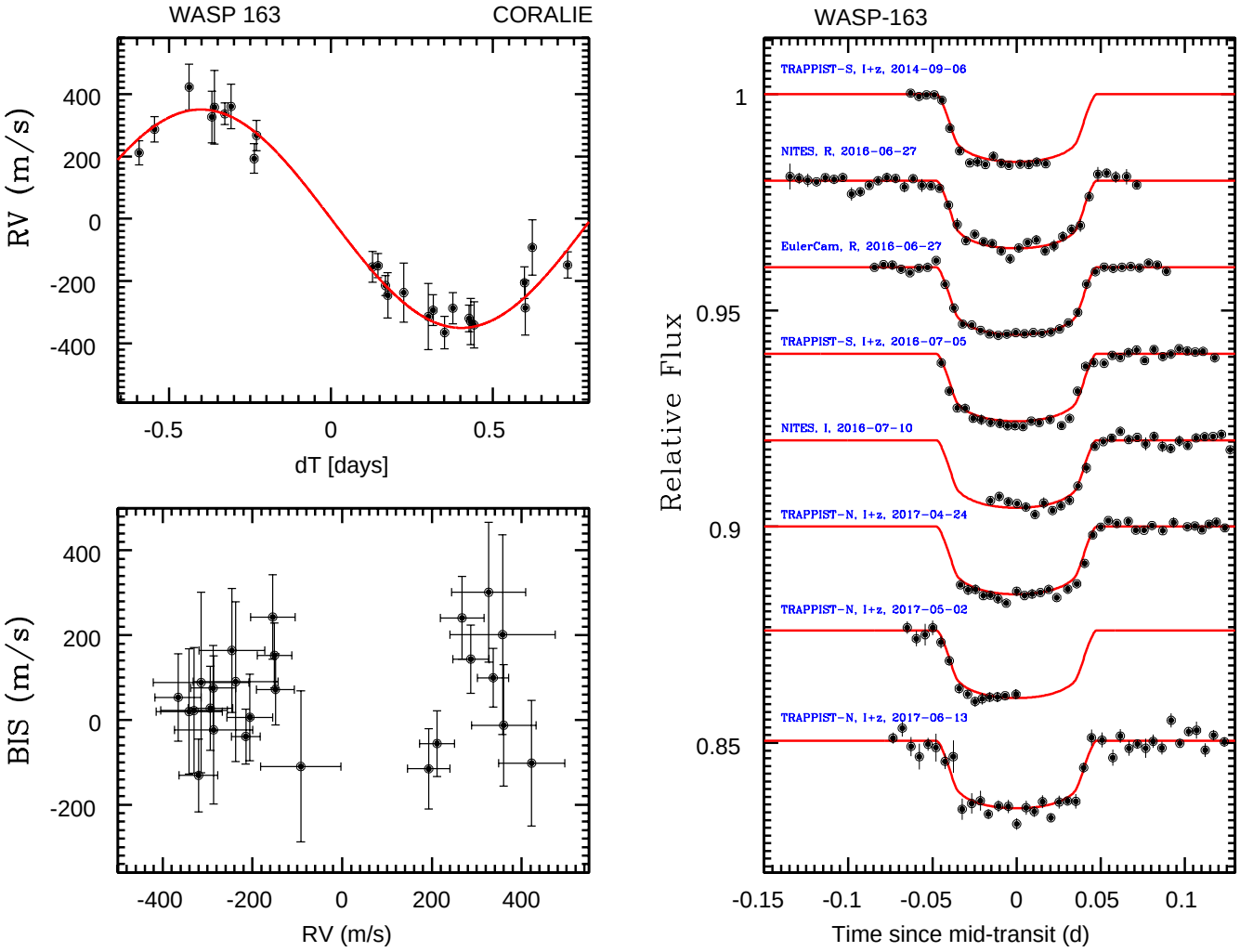

Figure 3. Same as Fig. 2 but for WASP-163.

$$M_{bol} = M_v + BC, \tag{2}$$

$$L_\star/L_\odot = 10^{0.4(4.74-M_{bol})}, \tag{3}$$

$$R_\star = L_\star/4\pi\sigma T_{eff}^4, \tag{4}$$

where M_v is the absolute visual magnitude, BC the bolometric correction (Pecaut and Mamajek 2013), d the distance in parsec pc, $L_\star$ is the star luminosity, and σ the Stefan-Boltzmann constant. We estimated the error on $R_\star$ by propagating the errors of all other parameters. We obtained 1.55 ± 0.08 $R_\odot$ for WASP-161, 0.86 ± 0.07 $R_\odot$ for WASP-163, and 0.91 ± 0.06 $R_\odot$ for WASP-170, in good agreement with our MCMC results shown in table 1.

4. STARS ROTATION PERIODS

Our photometric and radial-velocity data will be available in the web site, http://cdsarc.u-strasbg.fr

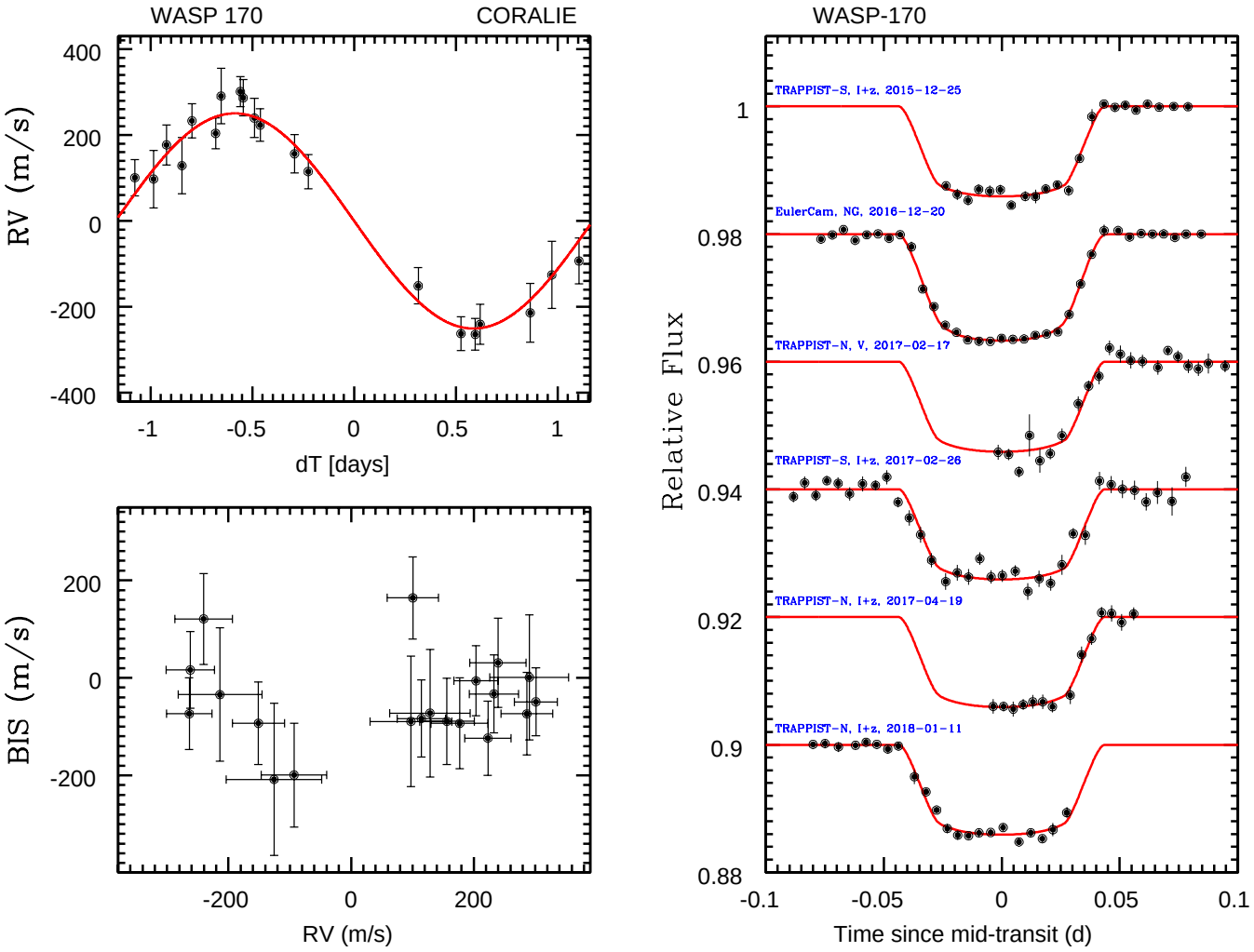

Figure 4. same as Fig. 2 but for WASP-170.

The WASP-170 light curve from WASP-South show a quasi-periodic modulation with an amplitude of about 0.6 % and a period of about 7.8 days. We assume this is due to the star spots (i.e. the combination of the star rotation and the magnetic activity). The rotational modulation of each star was estimated by using the sine-wave fitting method described in Maxted et al. (2011). The star variability due to star spots is not expected to be coherent on long time-scales as a consequence of the finite lifetime of the stars spots and differential rotation in the photosphere so we analyzed the WASP-170 data separately. We analyzed separately the WASP-170 data from each camera used, so that we can estimate the reliability of the results. The transit signal was removed from the data to calculating the periodograms by subtracting a simple transit model from the light curve. We calculated the periodograms over uniformly spaced frequencies from 0 to 1.5 cycles/day. The False Alarm Probability (FAP) is calculated by the bootstarp Monte Carlo as described in Maxted et al. (2011). The results are presented in the table 2, and the periodograms and light curves are shown in the figure 5. The rotation period value we obtain is $P_{rot} = 7.75 \pm 0.02$ days from the clear signal near 7.8 days in 5 out of 7 data sets. From the stellar radius estimated and rotation period implies the value of $V_{rot} \sin I = 6.1 \pm 0.3$ km s^{-1}, assuming that the axises of the star and the planet orbital are approximately aligned, in the good agreement with our spectroscopic analysis ($vsini = 5.6 \pm 1.0$ km s^{-1}, see the table 1). We

modeled the rotational modulation in the light curves for each camera and season with the rotation period fixed at $P_{rot} = 7.75$ d using the least-squares fit of a sinusoidal function and its first harmonic. Similar analysis for WASP-161 and WASP-163.

Camera	Dates (JD-2450000)	N	P [d]	a [mmag]	FAP
227	4846-4943	4899	7.780	0.010	$< 10^{-4}$
227	5567-5675	2407	3.978	0.005	0.15
227	5913-6041	2794	7.725	0.007	$< 10^{-4}$
228	4846-4943	5283	7.703	0.011	$< 10^{-4}$
228	5212-5308	4747	7.813	0.006	0.002
228	5613-5676	2651	4.073	0.003	1.00
228	5913-6041	3649	7.747	0.008	$< 10^{-4}$

Table 2. Periodogram analysis of the WASP light curves for WASP-170. N: the number of observations used in our analysis, a: the semi-amplitude of the best-fit sine wave at the period P found in the periodogram with false-alarm probability FAP.

5. STELLAR EVOLUTION MODELING

We estimated the mass and age of the host stars using the software *BAGEMASS*[1] based on the Bayesian method described in Maxted et al. (2015). The models used in the software *BAGEMASS* were calculated using the *GARSTEC* stellar evolution code as described in Weiss and Schlattl (2008). The deduced stellar masses and ages calculated are shown in the table 4. The inferred masses are in good agreement with the ones resulting from our global MCMC analysis (see Table 1).

6. DISCUSSION

WASP-161 b, WASP-163 b and WASP-170 b are planets slightly larger (1.14 ± 0.06 R_{Jup}, 1.2 ± 0.1 R_{Jup}, and 1.10 ± 0.09 R_{Jup}) and more massive (2.5 ± 0.2 M_{Jup}, 1.9 ± 0.2 M_{Jup}, and 1.6 ± 0.2 M_{Jup}) than Jupiter. Given their masses and their large irradiations (Fig. 6 **a**), their radii are well reproduced by the models of Fortney et al. (2007), assuming a core mass of a few dozens of $M_\oplus$ and ages larger than a few hundreds Myr (Fig. 6 **b**).

The empirical relationship derived by Weiss et al. (2013) for planets more massive than $150 M_\oplus$, $R_p/R_\oplus = 2.45(M_p/M_\oplus)^{-0.039\pm0.01}(F/\mathrm{erg\ s^{-1}cm^{-2}})^{0.094}$ predicts radii of 1.16 ± 0.30 R_{Jup}, 1.20 ± 0.34 R_{Jup} and 1.15 ± 0.31 R_{Jup} for WASP-161 b, 163 b, and 170 b, respectively, which are consistent with our measured radii. The three new planets whose discovery is described appear thus to be 'standard' hot Jupiters that do not present a 'radius anomaly' challenging standard models of irradiated gas giants.

The discovery of WASP-161 b, WASP-163 b, and WASP-170 b establishes the new robotic telescope TRAPPIST-North as a powerful Northern facility for the photometric follow-up of transiting exoplanet candidates found by ground-based wide-field surveys like WASP, and soon by the space-based mission TESS (Ricker et al. 2016).

7. ACKNOWLEDGEMENT

WASP-South is hosted by the SAAO and we are grateful for their ongoing support and assistance. Funding for WASP comes from consortium universities and from the UK's Science and Technology Facilities Council. The Euler-Swiss telescope is supported by the Swiss National Science Foundation. TRAPPIST-South is funded by the Belgian Fund for Scientic Research (FNRS) under the grant FRFC 2.5.594.09.F, with the participation of the Swiss National Science Foundation (SNF). MG is FNRS Research Associate, and EJ is FNRS Senior Research Associate. LD acknowledges support from the Gruber Foundation Fellowship. The research leading to these results has received funding from the European Research Council under the FP/2007-2013 ERC Grant Agreement 336480, and from the ARC grant for Concerted Research Actions, financed by the Wallonia-Brussels Federation. This work was also partially supported by a grant from the Simons Foundation (ID 327127 to Didier Queloz), a grant from the Erasmus+ International Credit Mobility programme (K Barkaoui), as well as by the MERAC foundation (PI Triaud).

[1] http://sourceforge.net/projects/bagemass

Target	Night	Telescope	Filter	N_p	T_{exp} (s)	Baseline function	σ (%)	$\sigma_{7.2m}$(%)	β_w	β_r	CF
WASP-161	2016-01-28	TRAPPIST-S	Sloan-z'	938	10	$p(t+xy+o)$	0.37	0.051	1.29	1.08	1.39
WASP-161	2017-12-20	TRAPPIST-N	Sloan-z'	902	10	$p(t+b)$	0.43	0.072	1.14	1.05	1.20
WASP-161	2018-01-05	SPECULOOS	Sloan-z'	1235	10	$p(xy)$	0.44	0.087	1.22	1.44	1.72
WASP-161	2018-02-12	TRAPPIST-N	Sloan-z'	892	10	$p(a)$	0.46	0.054	1.14	1.20	1.37
WASP-163	2014-09-06	TRAPPIST-S	$I+z$	345	12	$p(t)$	0.33	0.006	1.06	1.00	1.06
WASP-163	2016-06-27	NITES	Johnson-R	443	30	$p(t)$	0.41	0.012	1.71	1.00	1.71
WASP-163	2016-06-27	EulerCam	RG	170	60	$p(t+f+b)$	0.11	0.005	1.20	1.10	1.31
WASP-163	2016-07-05	TRAPPIST-S	$I+z$	602	12	$p(a+xy)$	0.35	0.011	1.16	1.35	1.56
WASP-163	2016-07-10	NITES	Johnson-I	388	30	$p(t)$	0.58	0.012	1.55	1.18	1.83
WASP-163	2017-04-24	TRAPPIST-N	$I+z$	487	12	$p(t+xy+o)$	0.31	0.008	1.02	1.07	1.09
WASP-163	2017-05-02	TRAPPIST-N	$I+z$	213	12	$p(b)$	0.54	0.009	0.90	1.00	0.90
WASP-163	2017-06-13	TRAPPIST-N	$I+z$	557	14	$p(t+f)$	0.69	0.021	0.87	1.16	1.01
WASP-170	2015-12-25	TRAPPIST-S	$I+z$	359	15	$p(f)$	0.29	0.008	1.04	1.05	1.09
WASP-170	2016-12-20	EulerCam	NGTS	207	40	$p(t)$	0.11	0.005	1.49	1.13	1.68
WASP-170	2017-02-17	TRAPPIST-N	Johnson-V	239	20	$p(t)$	0.46	0.013	1.22	1.00	1.22
WASP-170	2017-02-26	TRAPPIST-S	$I+z$	545	15	$p(t+a)$	0.51	0.015	1.32	1.16	1.53
WASP-170	2017-04-19	TRAPPIST-N	$I+z$	186	15	$p(a+xy)$	0.41	0.008	0.99	1.00	0.99
WASP-170	2018-01-11	TRAPPIST-N	$I+z$	315	15	$p(t)$	0.26	0.007	0.75	1.11	0.83

Table 3. The table shows for each light curve the date , telescope, filter, number of data points, the exposure time, the selected baseline function, the RMS of the best-fit residuals, the deduced values for β_w, β_r and $CF = \beta_w \times \beta_r$. For the baseline function, $p(\epsilon^N)$, denotes, respectively, a $N-$order polynomial function of time ($\epsilon = t$), airmass ($\epsilon = a$), full-width at half maximum ($\epsilon = f$), background ($\epsilon = b$), and x and y positions ($\epsilon = xy$). The symbol o demotes an offset fixed at the time of the meridian flip.

Table 4. Stellar mass and age estimates from the software *BAGEMASS*.

Star	Mass [$M_\odot$]	Age [Gyr]
WASP-161 A	1.42 ± 0.05 (1.40)	2.4 ± 0.4 (2.4)
WASP-163 A	0.87 ± 0.06 (0.78)	11.4 ± 3.5 (17.4)†
WASP-170 A	0.99 ± 0.07 (1.03)	4.8 ± 3.1 (2.9)

† Best fit occurs at edge of model grid.

REFERENCES

Mayor, M.; Queloz, D. *Nature* **1995**, *378*, 355–359.

Charbonneau, D.; Brown, T. M.; Latham, D. W.; Mayor, M. *ApJL* **2000**, *529*, L45–L48.

Henry, G. W.; Marcy, G. W.; Butler, R. P.; Vogt, S. S. *ApJL* **2000**, *529*, L41–L44.

Winn, J. N.; Fabrycky, D. C. *ARA&A* **2015**, *53*, 409–447.

Fortney, J. J.; Marley, M. S.; Barnes, J. W. *ApJ* **2007**, *659*, 1661–1672.

Correia, A. C. M.; Laskar, J. *Icarus* **2010**, *205*, 338–355.

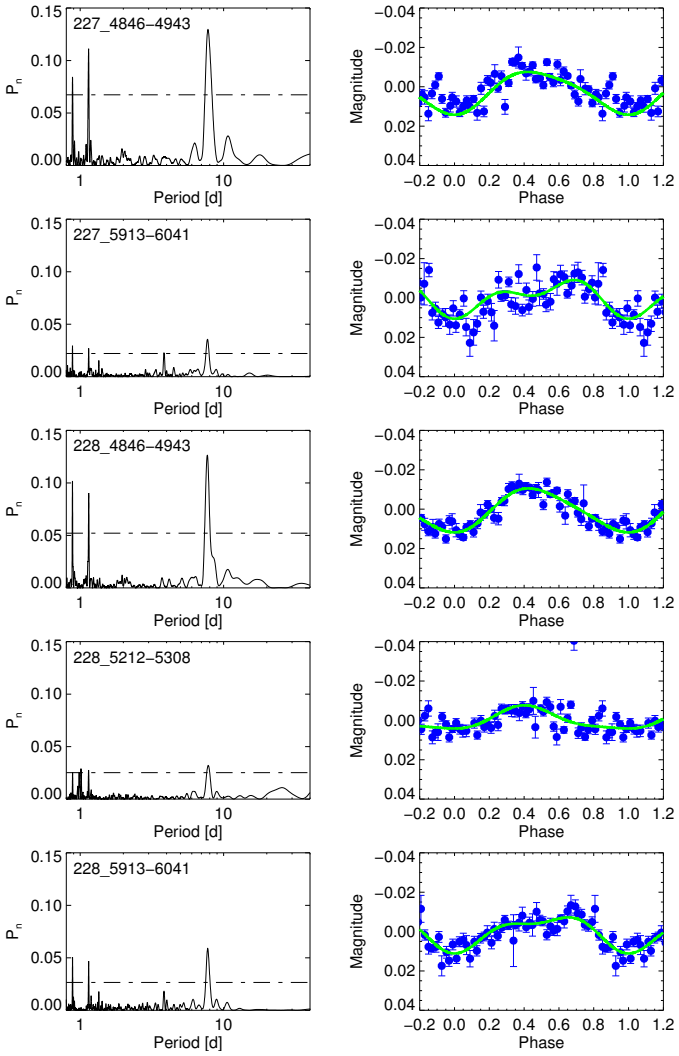

Figure 5. *Left panel*: Periodograms of WASP-170. Horizontal lines indicate false-alarm probability levels 0.1, 0.01 and 0.001. *Right panel*: Light curves binned in the blue points on the assumed rotation period of 7.75 days with second-order harmonic series fit by least squares in the green lines.

LD coefficient	WASP-161	WASP-163	WASP-170
$u_{1,z'}$	0.184 ± 0.011	-	-
$u_{2,z'}$	0.300 ± 0.005	-	-
$u_{1,I+z}$	-	0.207 ± 0.012	0.2539 ± 0.0202
$u_{2,I+z}$	-	0.297 ± 0.010	0.2788 ± 0.0152
$u_{1,Johnson-I}$	-	0.331 ± 0.034	0.2727 ± 0.0321
$u_{2,Johnson-I}$	-	0.251 ± 0.019	0.2805 ± 0.0158
$u_{1,Johnson-R}$	-	0.420 ± 0.043	-
$u_{2,Johnson-R}$	-	0.248 ± 0.027	-
$u_{1,Johnson-V}$	-	-	0.437 ± 0.044
$u_{2,Johnson-V}$	-	-	0.271 ± 0.025

Table 5. The quadratic limb-darkening (LD) coefficients u_1 and u_2 used in our MCMC analysis.

Chang, C.; Liu, G. Z.; Tang, C. X.; Chen, C. H.; Shao, H.; Huang, W. H. *Applied Physics Letters* **2010**, *96*, 111502.

Winn, J. N. *ArXiv e-prints* **2010**,

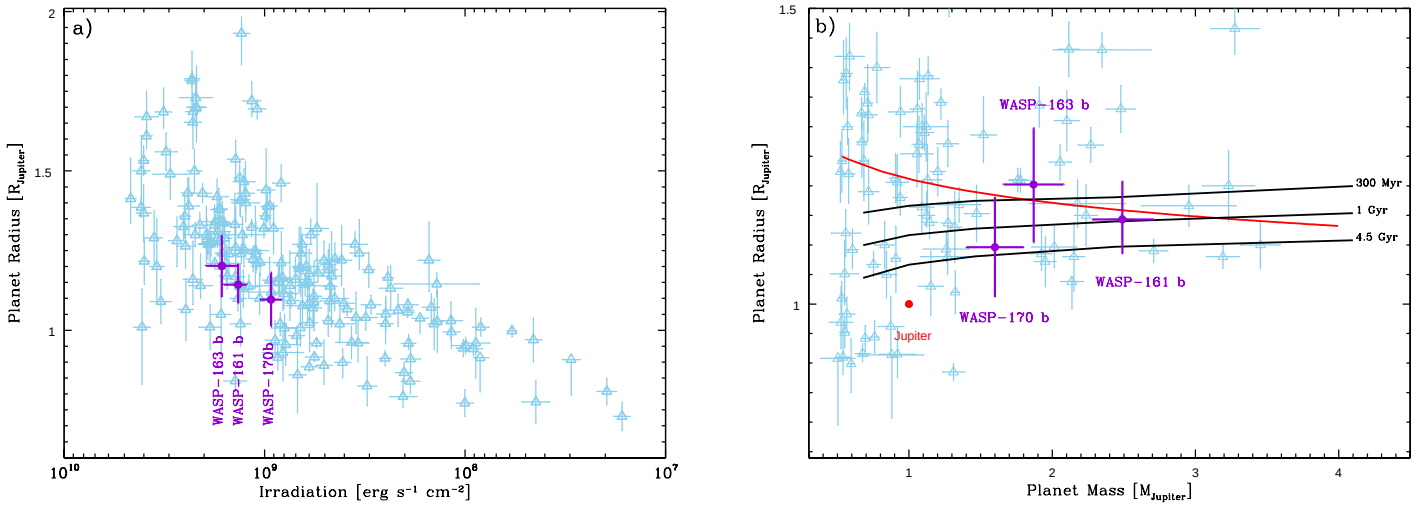

Figure 6. a): Irradiation-radius diagram and **b)**: mass-radius diagram for the known transiting planets with masses ranging from 0.5 to 4 $M_{Jupiter}$ (data from exoplanets.org are shown as skyblue triangles with error bars). The planets WASP-161 b, WASP-163 b and WASP-170 b are shown in violet. In **b)** the black lines present models of irradiated giant planets with semi-major axes of 0.045 AU, core masses of 25 $M_{\oplus}$, and ages of 300 Myrs, 1 Gyrs and 4.5 Gyrs (Fortney et al. 2007). The empirical law of Weiss et al. (2013) is also plotted as a red line.

Deming, D.; Seager, S. *Nature* **2009**, *462*, 301–306.

Seager, S.; Deming, D. *ARA&A* **2010**, *48*, 631–672.

Sing, D. K. et al. *Nature* **2016**, *529*, 59–62.

Crossfield, I. J. M. *PASP* **2015**, *127*, 941.

Pollacco, D. L. et al. *Publications of the Astronomical Society of the Pacific* **2006**, *118*, 1407–1418.

Collier Cameron, A. et al. *MNRAS* **2007**, *380*, 1230–1244.

Hellier, C.; Anderson, D. R.; Collier-Cameron, A.; Miller, G. R. M.; Queloz, D.; Smalley, B.; Southworth, J.; Triaud, A. H. M. J. *ApJL* **2011**, *730*, L31.

Hellier, C. et al. *MNRAS* **2012**, *426*, 739–750.

Collier Cameron, A. et al. *MNRAS* **2006**, *373*, 799–810.

Collier Cameron, A. et al. *MNRAS* **2007**, *380*, 1230–1244.

Gillon, M. et al. *Nature* **2017**, *542*, 456–460.

Gillon, M. *Nature Astronomy* **2018**, *2*, 344–344.

Burdanov, A.; Delrez, L.; Gillon, M.; Jehin, E.; Speculoos, T.; Trappist Teams, *Handbook of Exoplanets, Edited by Hans J. Deeg and Juan Antonio Belmonte. Springer Living Reference Work, ISBN: 978-3-319-30648-3, 2017, id.130*; 2017; p 130.

Delrez, L. et al. *ArXiv e-prints* **2018**,

Bonfils, X.; Gillon, M.; Forveille, T.; Delfosse, X.; Deming, D.; Demory, B.-O.; Lovis, C.; Mayor, M.; Neves, V.; Perrier, C.; Santos, N. C.; Seager, S.; Udry, S.; Boisse, I.; Bonnefoy, M. *A&A* **2011**, *528*, A111.

Gillon, M. et al. *A&A* **2012**, *542*, A4.

Delrez, L. et al. *A&A* **2014**, *563*, A143.

Jehin, E.; Gillon, M.; Queloz, D.; Magain, P.; Manfroid, J.; Chantry, V.; Lendl, M.; Hutsemékers, D.; Udry, S. *The Messenger* **2011**, *145*, 2–6.

Gillon, M. et al. *A&A* **2013**, *552*, A82.

Gillon, M.; Jehin, E.; Magain, P.; Chantry, V.; Hutsemékers, D.; Manfroid, J.; Queloz, D.; Udry, S. *EPJ Web of Conferences* **2011**, *11*, 06002.

Lendl, M. et al. *Astronomy & Astrophysics* **2012**, *544*, A72.

Wheatley, P. J. et al. *ArXiv e-prints* **2017**,

McCormac, J.; Skillen, I.; Pollacco, D.; Faedi, F.; Ramsay, G.; Dhillon, V. S.; Todd, I.; Gonzalez, A. *Monthly Notices of the Royal Astronomical Society* **2014**, *438*, 3383–3398.

Craig, M. W. et al. ccdproc: CCD data reduction software. Astrophysics Source Code Library, 2015.

Barbary, K. *The Journal of Open Source Software* **2016**, *1*, 1.

Bertin, E.; Arnouts, S. *A&AS* **1996**, *117*, 393–404.

McCormac, J.; Pollacco, D.; Skillen, I.; Faedi, F.; Todd, I.; Watson, C. A. *PASP* **2013**, *125*, 548.

Queloz, D.; Mayor, M.; Naef, D.; Santos, N.; Udry, S.; Burnet, M.; Confino, B. **2000**, 548.

Baranne, A.; Queloz, D.; Mayor, M.; Adrianzyk, G.; Knispel, G.; Kohler, D.; Lacroix, D.; Meunier, J.-P.; Rimbaud, G.; Vin, A. *A&AS* **1996**, *119*, 373–390.

Queloz, D.; Henry, G. W.; Sivan, J. P.; Baliunas, S. L.; Beuzit, J. L.; Donahue, R. A.; Mayor, M.; Naef, D.; Perrier, C.; Udry, S. *A&A* **2001**, *379*, 279–287.

Target	HID - 2,450,000	RV (km s^{-1})	σ_{RV} (km s^{-1})	BS (km s^{-1})	Target	HID - 2,450,000	RV (km s^{-1})	σ_{RV} (km s^{-1})	BS (km s^{-1})
WASP-163	7193.741864	-37.28368	0.11764	-0.05553	WASP-161	6995.779435	37.47673	0.03954	0.10140
WASP-163	7194.544082	-37.93075	0.07383	0.14349	WASP-161	7404.735111	37.93140	0.04051	-0.15260
WASP-163	7221.642393	-37.90136	0.07320	-0.10196	WASP-161	7421.604076	37.83967	0.03886	-0.17254
WASP-163	7264.560197	-37.21532	0.08258	0.30132	WASP-161	7422.600890	37.60262	0.03490	-0.17929
WASP-163	7265.528948	-37.85780	0.08717	0.20131	WASP-161	7423.668930	37.52064	0.03555	-0.28021
WASP-163	7268.579849	-37.96344	0.07401	0.09958	WASP-161	7425.646222	37.72356	0.03456	-0.04948
WASP-163	7276.497340	-37.95927	0.10641	-0.01258	WASP-161	7426.579130	37.96837	0.03946	-0.16563
WASP-163	7277.497313	-37.30844	0.07177	-0.11522	WASP-161	7428.627488	37.41733	0.03252	0.04443
WASP-163	7292.517764	-37.82511	0.09442	0.24068	WASP-161	7451.572650	37.47357	0.03171	-0.18188
WASP-163	7293.464761	-37.14368	0.07405	0.24267	WASP-161	7452.635935	37.57245	0.03459	0.02944
WASP-163	7294.524814	-37.73113	0.08910	0.15248	WASP-161	7453.567361	37.93838	0.03395	-0.14701
WASP-163	7484.863204	-37.46746	0.03879	-0.03903	WASP-161	7457.538982	37.46129	0.03590	0.10144
WASP-163	7486.827998	-37.42444	0.04741	0.16399	WASP-161	7481.604825	37.65253	0.04218	-0.16457
WASP-163	7487.796538	-37.79839	0.04198	0.09038	WASP-161	7485.611602	37.80633	0.03723	0.06739
WASP-163	7488.843232	-37.86941	0.03227	0.08838	WASP-161	7669.874869	37.96450	0.03643	-0.26075
WASP-163	7523.858463	-37.41079	0.04884	0.02768	WASP-161	7670.873488	37.54791	0.03644	0.07926
WASP-163	7567.695488	-37.80440	0.03823	0.05318	WASP-161	7674.868344	37.89486	0.04877	-0.13512
WASP-163	7569.757824	-37.85478	0.05104	0.07520	WASP-161	7716.752403	37.48642	0.06487	-0.04681
WASP-163	7575.726750	-37.81565	0.04977	-0.13093	WASP-161	7717.747923	37.75662	0.04854	-0.01920
WASP-163	7576.662344	-37.38270	0.04033	0.02235	WASP-161	7718.788841	37.80035	0.03818	-0.07805
WASP-163	7577.523403	-37.95890	0.04961	0.01980	WASP-161	7726.778064	37.39224	0.03876	0.01718
WASP-163	7593.681424	-37.95775	0.05024	0.00629	WASP-161	7746.846331	37.51936	0.03845	-0.04507
WASP-163	7652.535369	-37.33184	0.03470	-0.02346	WASP-161	7751.735303	37.69111	0.05137	-0.11653
WASP-163	7823.841592	-38.04752	0.05155	-0.10981	WASP-161	7761.696319	37.93171	0.04203	-0.35162
WASP-163	7894.742995	-37.97268	0.04302	0.07214					
WASP-170	7066.749515	30.67098	0.04671	0.16402	WASP-170	7753.676136	30.70862	0.03924	-0.12366
WASP-170	7686.843189	31.25138	0.06427	-0.08954	WASP-170	7754.698984	31.19850	0.04009	-0.08925
WASP-170	7694.846421	30.81621	0.04224	-0.09353	WASP-170	7759.695126	31.20223	0.04579	-0.08356
WASP-170	7719.778573	31.25569	0.04232	-0.07239	WASP-170	7760.780900	30.70044	0.03683	-0.09317
WASP-170	7721.746763	31.13284	0.04660	-0.03291	WASP-170	7773.792434	31.17400	0.03803	0.01621
WASP-170	7723.773046	30.84403	0.05319	-0.00621	WASP-170	7801.545185	31.08175	0.06548	-0.07362
WASP-170	7724.787756	31.05367	0.03945	0.00095	WASP-170	7812.635803	30.67711	0.06835	0.12073
WASP-170	7726.799025	31.25678	0.03495	-0.04931	WASP-170	7825.546120	31.14228	0.04425	-0.03448
WASP-170	7747.780705	31.16081	0.03596	-0.07385	WASP-170	7859.637199	30.88820	0.07800	-0.20830
WASP-170	7749.729288	31.01646	0.04208	0.03075	WASP-170	7883.473343	31.07842	0.06692	-0.19927

Table 6. CORALIE radial-velocity measurements for WASP-161, WASP-163 and WASP-170 (BS = bisector spans).

Torres, G.; Konacki, M.; Sasselov, D. D.; Jha, S. *ApJ* **2004**, *614*, 979–989.

Doyle, A. P.; Smalley, B.; Maxted, P. F. L.; Anderson, D. R.; Cameron, A. C.; Gillon, M.; Hellier, C.; Pollacco, D.; Queloz, D.; Triaud, A. H. M. J.; West, R. G. *MNRAS* **2013**, *428*, 3164–3172.

Doyle, A. P.; Davies, G. R.; Smalley, B.; Chaplin, W. J.; Elsworth, Y. *MNRAS* **2014**, *444*, 3592–3602.

Murray, C. D.; Correia, A. C. M. In *Exoplanets*; Seager, S., Ed.; 2010; pp 15–23.

Mandel, K.; Agol, E. *ApJL* **2002**, *580*, L171–L175.

Schwarz, G. *Ann. Statist.* **1978**, *6*, 461–464.

Claret, A. *VizieR Online Data Catalog* **2000**, *336*.

Gelman, A.; Rubin, D. B. *Statistical Science* **1992**, *7*, 457–472.

Enoch, B.; Collier Cameron, A.; Parley, N. R.; Hebb, L. *A&A* **2010**, *516*, A33.

Gaia Collaboration,; Brown, A. G. A.; Vallenari, A.; Prusti, T.; de Bruijne, J. H. J.; Babusiaux, C.; Bailer-Jones, C. A. L.; Biermann, M.; Evans, D. W.; Eyer, L.; et al., *A&A* **2018**, *616*, A1.

Pecaut, M. J.; Mamajek, E. E. *ApJS* **2013**, *208*, 9.

Maxted, P. F. L. et al. *PASP* **2011**, *123*, 547.
Maxted, P. F. L.; Serenelli, A. M.; Southworth, J. *A&A* **2015**, *575*, A36.
Weiss, A.; Schlattl, H. *Ap&SS* **2008**, *316*, 99–106.
Weiss, L. M. et al. *ApJ* **2013**, *768*, 14.
Ricker, G. R. et al. The Transiting Exoplanet Survey Satellite. Space Telescopes and Instrumentation 2016: Optical, Infrared, and Millimeter Wave. 2016; p 99042B.